


Ventricular mass discriminates pulmonary arterial hypertension as redefined at the Sixth World Symposium on Pulmonary Hypertension

Catherine E. Simpson¹  | Todd M. Kolb¹ | Steven Hsu² |
Stefan L. Zimmerman³ | Celia P. Corona-Villalobos⁴ | Stephen C. Mathai¹ |
Rachel L. Damico¹ | Paul M. Hassoun¹

¹Department of Medicine, Division of Pulmonary and Critical Care Medicine, Johns Hopkins University, Baltimore, Maryland, USA

²Department of Medicine, Division of Cardiology, Johns Hopkins University, Baltimore, Maryland, USA

³Department of Radiology and Radiological Science, Johns Hopkins University, Baltimore, Maryland, USA

⁴Department of Medicine, Division of Nephrology, Johns Hopkins University, Baltimore, Maryland, USA

Correspondence

Rachel L. Damico and Paul M. Hassoun, Department of Medicine, Division of Pulmonary and Critical Care Medicine, Johns Hopkins University, Baltimore, MD 21205, USA.

Email: rdamico1@jhmi.edu and phassou1@jhmi.edu

Funding information

National Heart, Lung, and Blood Institute, Grant/Award Numbers: K23HL153781, P50 HL084946, R01HL114910, U01HL125175

Abstract

Cardiac magnetic resonance (CMR) measures of right ventricular (RV) mass, volumes, and function have diagnostic and prognostic value in pulmonary arterial hypertension (PAH). We hypothesized that RV mass-based metrics would discriminate incident PAH as redefined by the lower mean pulmonary arterial pressure (mPAP) threshold of >20 mmHg at the Sixth World Symposium on Pulmonary Hypertension (6th WSPH). Eighty-nine subjects with suspected PAH underwent CMR imaging, including 64 subjects with systemic sclerosis (SSc). CMR metrics, including RV and left ventricular (LV) mass, were measured. All subjects underwent right heart catheterization (RHC) for assessment of hemodynamics within 48 h of CMR. Using generalized linear models, associations between CMR metrics and PAH were assessed, the best subset of CMR variables for predicting PAH were identified, and relationships between mass-based metrics, hemodynamics, and other predictive CMR metrics were examined. Fifty-nine subjects met 6th WSPH criteria for PAH. RV mass metrics, including ventricular mass index (VMI), demonstrated the greatest magnitude difference between subjects with versus without PAH. Overall and in SSc, VMI and RV mass measured by CMR were among the most predictive variables discriminating PAH at RHC, with areas under the receiver operating characteristic curve 0.86 and 0.83, respectively. VMI increased linearly with pulmonary vascular resistance and with mPAP in PAH, including in lower ranges of mPAP associated with mild PAH. $VMI \geq 0.37$ yielded a positive predictive value of 90% for discriminating PAH. RV mass metrics measured by CMR, including VMI, discriminate incident, treatment-naïve PAH as defined by 6th WSPH criteria.

KEYWORDS

diagnosis, magnetic resonance imaging, pulmonary hypertension

*Dr. Damico and Hassoun contributed equally.

This is an open access article under the terms of the Creative Commons Attribution-NonCommercial License, which permits use, distribution and reproduction in any medium, provided the original work is properly cited and is not used for commercial purposes.

© 2021 The Authors. *Pulmonary Circulation* published by John Wiley & Sons Ltd on behalf of Pulmonary Vascular Research Institute.

INTRODUCTION

PAH is a progressive disease of the pulmonary vasculature that leads to RV failure and premature death.^{1,2} Because RV failure is the leading cause of mortality in PAH, noninvasive methods of assessing RV structure and function have been investigated for utility in defining PAH risk and predicting outcomes.^{3–7} CMR, with its three-dimensional imaging and high interobserver reproducibility, has emerged as a powerful tool for assessing the RV.^{8,9} Several recent meta-analyses have revealed elevated RV volumes, reflective of RV dilation, and decreased right ventricular ejection fraction (RVEF), reflective of RV dysfunction, to be the most well-established CMR measurements with consistently demonstrated prognostic value in known PAH.^{10–12}

Fewer studies, however, have examined the ability of CMR metrics to discriminate the presence of hemodynamically confirmed PAH in patients at risk or suspected of the disease. Studies that have examined this question have shown increased RV mass, reflective of RV hypertrophy, predicts the presence of disease in subjects with suspected PAH. In particular, VMI, a ratio of RV mass to left ventricular (LV) mass that reflects the effects of PAH on both RV and LV remodeling,^{13–16} has been consistently found discriminating of PAH. Other CMR metrics shown to discriminate PAH include relative area change of the pulmonary artery, displacement of the interventricular septum during the cardiac cycle, and black blood slow flow, parameters which are not routinely incorporated into CMR protocols.^{14,17,18}

Recently, PAH has been redefined to include patients with mean pulmonary artery pressures (mPAP) greater than 20 mmHg.² This change was brought about by increasing recognition that normal pulmonary artery pressures are significantly lower than the prior diagnostic threshold of 25 mmHg, and that patients with mild elevations in mPAP suffer worse outcomes than patients with normal pulmonary artery pressures.^{19,20} Only one published letter has reported CMR associations with PAH using this lower threshold for diagnosis, and no studies have examined relationships between predictive CMR metrics and ranges of mPAP consistent with mild disease.²¹ Whether patients with mPAP of 21–24 mmHg stand to benefit from earlier initiation of PAH-specific therapies remains to be determined, however, there is evidence to support better outcomes with early diagnosis of milder disease.^{22,23}

In the current study, we sought to identify CMR metrics that differ significantly between subjects with versus without PAH using the new, lower mPAP threshold of >20 mmHg in a prospective cohort referred for RHC on the basis of suspected disease. Given the

usual progression of RV changes in response to increased afterload, whereby RV hypertrophy precedes dilatation and dysfunction, we hypothesized that increased VMI would be an early, sensitive indicator of mild PAH. Because patients with SSc represent the largest population of at-risk patients who undergo routine PAH screening, we also sought to identify discriminating CMR parameters in the subgroup of patients with SSc.

METHODS

Patient enrollment

This prospective cohort study was approved by the Johns Hopkins University Institutional Review Board (NA_00027124, Baltimore, MD), and written informed consent was obtained for all patients. Eighty-nine subjects suspected of having PAH by their physicians were recruited by the Johns Hopkins Pulmonary Hypertension Program (JHPHP) between July 2007 and September 2014. The presence of SSc was determined by expert opinion according to American College of Rheumatology (ACR) 1980 criteria for patients enrolled through 2013, after which revised ACR/European League against Rheumatism classification criteria were applied. Subjects with SSc were referred to the JHPHP on the basis of previously published criteria.^{24,25} All subjects with suspected PAH underwent CMR within 48 h of an RHC that defined hemodynamics according to a predefined study protocol and identified the presence or absence of disease. For these analyses, in accordance with the hemodynamic criteria adopted at the 6th WSPH, PAH was defined as mPAP > 20 mmHg with PVR \geq 3 Wood units and pulmonary capillary wedge pressure \leq 15 mmHg, in the absence of other known causes of PH.²

Image acquisition and interpretation

CMR was performed on a 3-T MRI system (Magnetom Trio, Siemens Healthcare) with subjects in the supine position, and images were interpreted using commercially available software (Qmass version 6.2.2 and Mass 5.1). CMR protocol included breath-hold cine short-axis and four-chamber image acquisition with retrospective gating at 3-T using a body coil array. Segmented gradient echo (FLASH) cine short-axis images of both ventricles were acquired from base to apex. Sequence parameters included repetition time/echo time (TR/TE) of 64.2/2.97 ms; slice thickness of 6 mm without gap; flip angle of 18°; and acquisition matrix of 256 \times 192. Cine four-chamber images were obtained with a retrospectively gated segmented

gradient-echo sequence (FLASH). Sequence parameters included TR/TE of 52.2/2.82 ms; slice thickness of 8 mm without gap; flip angle of 12°; and acquisition matrix of 256 × 192. Radiologists with expertise in CMR interpretation (S. L. Z. and C. P. C. -V.) obtained standard LV and RV functional and volumetric parameters with three-dimensional measures using contiguous short-axis cine images covering the entire RV and LV. The RV and LV epicardial and endocardial ventricular borders were manually traced in end-systole (ES) and end-diastole (ED) (Figure 1). Trabeculations were excluded from the endocardial ventricular border definition at ED and included in the border definition at ES. The interventricular septum was excluded from the RV mass and included in the LV mass. For methodologic alignment with prior literature, RV delineations at ED were used for RV mass in our analyses, with measurements at ES examined in exploratory analyses. Ejection fraction was calculated for RV and LV. RV and LV mass were measured according to the following equation: ventricular mass = 1.05 (epicardial volume – endocardial volume). Tricuspid annular plane systolic excursion (TAPSE) was calculated by measuring the displacement of the lateral tricuspid valve annulus toward the apex between ED and ES phases, as previously delineated by our group.²⁶ RV fractional shortening (RVFS) was calculated as (TAPSE/ED – annulus to apex length) × 100. RV fractional area change (RVFAC) assessment was performed using cine four-chamber images by measuring percentage change as follows: $RVFAC = (ED - RV \text{ area} - ES - RV \text{ area}) / (ED - RV \text{ area}) \times 100$. CMR metrics, including ED and ES volumes, stroke volume, CO, and ventricular mass, were indexed to body surface area for each subject. VMI was calculated by dividing RV ED mass by LV EDC mass.^{13,26,27}

Statistical analysis

Patient demographics and clinical variables were summarized using descriptive statistics. Normality of CMR measure distributions was assessed using the Shapiro–Wilk test. Comparisons of metrics between subjects with versus without PAH were made using fold-change analyses and unpaired *t* tests or Mann–Whitney tests, as appropriate. ROC curves were constructed to characterize the ability of VMI and other metrics to discriminate PAH based on the area under the curve (AUC). Simple and multivariable logistic regressions were performed to examine relationships between CMR metrics that differed in PAH and the odds of disease presence. Variables were scaled to $\log_{1.1}$ for regression to facilitate direct comparison of effect sizes. CMR metrics with previously demonstrated diagnostic or prognostic value in PAH were incorporated into multivariable logistic models. The best subsets predictors of the presence of PAH were selected using Akaike Information Criteria and incorporated into final predictive models to describe the odds of PAH. Regression diagnostics were performed using Hosmer–Lemeshow and Pearson goodness of fit tests, and collinearity of predictors was assessed using variance inflation factors. Final logistic models were internally cross-validated using leave-one-out cross-validation. Sensitivity and specificity of VMI cut points were explored. Relationships between VMI, RV loading conditions (represented by mPAP and PVR), and other CMR metrics predictive of PAH in logistic models were examined using scatter plots with lowess smoothing and linear regression models with generation of spline terms for assessing nonlinear relationships. All statistical analyses were performed using Stata version 15.1 (StataCorp). A *p* < 0.05 was considered statistically significant.

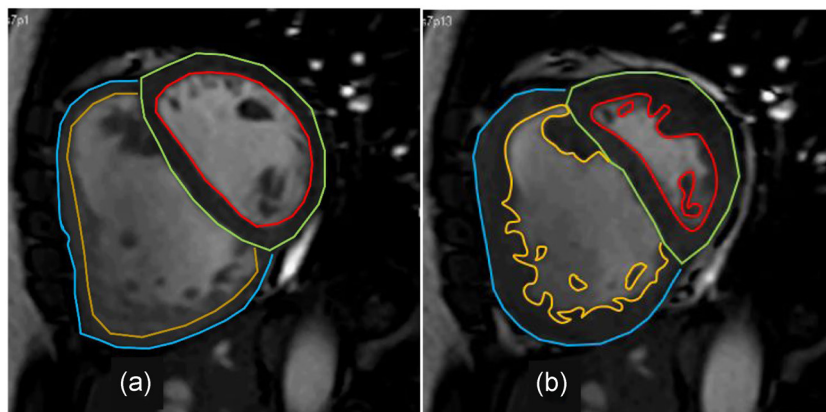


FIGURE 1 Manual endo- and epicardial contouring of the right and left ventricles in end-diastole (panel a) and end-systole (panel b) from a cine short-axis cardiac magnetic resonance image acquisition in a patient diagnosed with systemic sclerosis-associated pulmonary arterial hypertension. Blue lines mark right ventricular (RV) epicardium; yellow lines mark RV endocardium; green lines mark left ventricular (LV) epicardium; and red lines mark LV endocardium

RESULTS

Eighty-nine subjects with suspected PAH underwent RHC within 48 h of CMR. Fifty-nine subjects met diagnostic criteria for PAH as defined by the 6th WSPH; 30 did not have PAH. Of the 59 with PAH, 19 subjects had mild PAH with $mPAP \leq 35$ mmHg, 25 had moderately elevated $mPAP > 35$ –50 mmHg, and 15 had severely elevated $mPAP > 50$ mmHg. Of the 30 subjects without PAH, 13 had no pulmonary hypertension, and 17 had $mPAP > 20$ mmHg, although without any evidence of pulmonary vascular disease (e.g., no precapillary component signified by $PVR \geq 3$) to satisfy criteria for PAH (Figure 2). Among those diagnosed with PAH, 39 were classified as having SSc-PAH, and 20 were judged to have idiopathic PAH.

Demographic and clinical characteristics for subjects with versus without PAH are presented in Table 1. Overall, subjects were mostly white and mostly female, with the majority having SSc. Subjects with PAH had higher proBNP levels, higher New York Heart Association functional classifications, and more adverse hemodynamics than patients without PAH. CMR measurements for subjects with and without PAH are shown

in Table 2. As expected, subjects with PAH had higher RV volumes and RV mass metrics and lower RV functional metrics. CMR measurements for subjects with PAH by disease severity (mild, moderate, or severe PAH) are shown in Table S1. Similarly, subjects with more severe disease had greater RV volumes and mass and worse RV function. Clinical characteristics and CMR measurements for subjects by disease subtype (SSc-PAH vs. IPAH) are shown in Tables S2 and S3. Subjects with SSc-PAH had worse walk distances and functional status compared to those with IPAH despite similar hemodynamics.

The volcano plots in Figure 3 show the magnitude of fold-change differences for CMR metrics between subjects with versus without PAH, and the significance of these differences after adjustment for multiple testing. In the overall cohort, VMI, RV mass measures, RV end-systolic volumes (RVESV), and RV mass to volume ratio (RVMVR) were significantly greater in subjects with PAH. Conversely, RVFS and RVEF were significantly lower in subjects with PAH (Figure 3a). Results were similar in the subset of subjects with SSc (Figure 3b). Fold-change differences for all CMR variables in the overall cohort (corresponding to Figure 3a) and in SSc

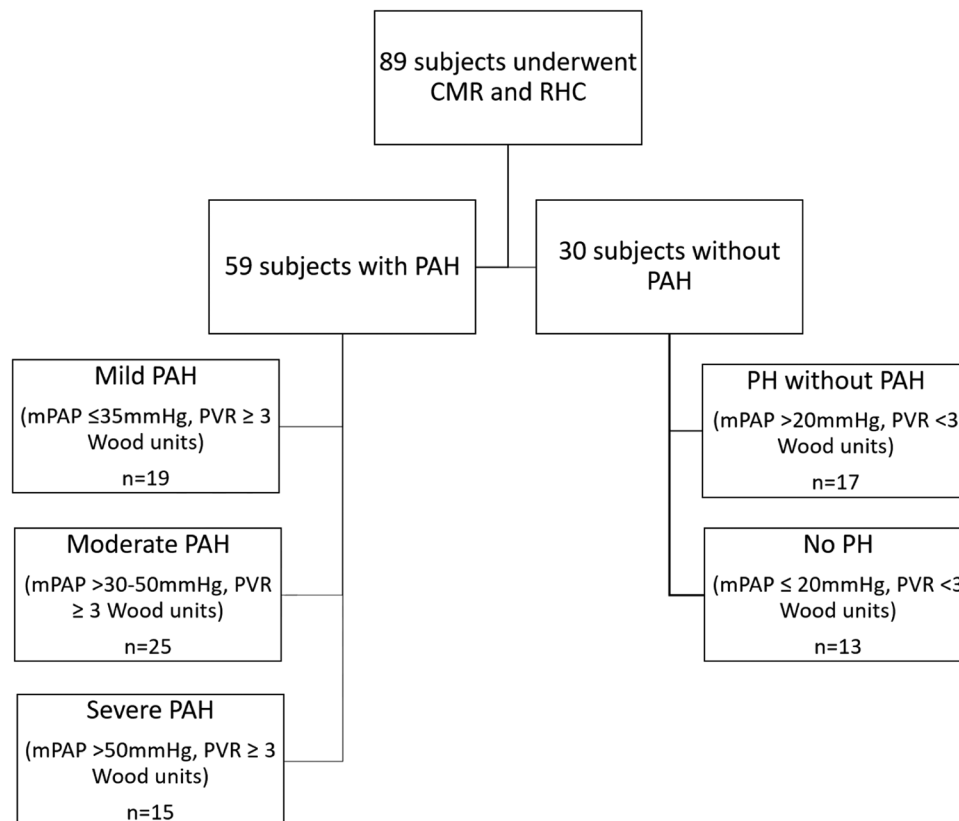


FIGURE 2 Diagram demonstrating the breakdown of subjects with versus without mild, moderate, or severe pulmonary arterial hypertension (PAH)

TABLE 1 Demographic and clinical characteristics of subjects with and without PAH

Observations, <i>n</i>	Characteristic	No PAH	PAH	<i>p</i> value
<i>Demographics</i>				
89	Subjects, <i>n</i>	30	59	
89	Age, years	61 (10)	57 (11)	0.20
89	Sex, <i>n</i> (% female)	22 (73)	54 (92)	0.02
89	Race, <i>n</i> (% White)	23 (77)	53 (90)	0.25
89	SSc, <i>n</i> (%)	25 (83)	39 (66)	0.09
89	BMI, kg/m ²	26 (4)	29 (8)	0.07
82	NYHA FC, <i>n</i> (%III/IV)	5 (17)	28 (47)	<0.01
77	6MWD, <i>m</i>	405 (124)	378 (131)	0.41
<i>Laboratory values</i>				
87	Cr, mg/dl (median, IQR)	0.8 (0.7, 0.9)	0.9 (0.7, 1.1)	0.24
75	proBNP, pg/ml (median, IQR)	139 (61, 276)	535 (261, 1757)	<0.01
<i>Hemodynamics</i>				
89	RAP, mmHg	5 (3)	8 (5)	<0.01
89	mPAP, mmHg	21 (5)	44 (13)	<0.01
89	PAWP, mmHg	9 (3)	10 (4)	0.50
89	PVR, wood units	2.2 (0.6)	8.6 (4.8)	<0.01
89	Cardiac output, L/min	5.2 (1.4)	4.4 (1.3)	0.01
89	Cardiac index, L/min/m ²	2.9 (0.6)	2.5 (0.7)	<0.01
88	PA Sat %	70.6 (4.5)	67.0 (7.4)	0.02

Note: All values reported as mean (SD) unless otherwise specified. *p* values correspond to significance testing of differences of means or medians as specified. Abbreviations: 6MWD, 6-min walk distance; BMI, body mass index; Cr, creatinine; mPAP, mean pulmonary arterial pressure; NYHA FC, New York Heart Association Functional Class; PA Sat, pulmonary artery saturation; PAWP, pulmonary artery wedge pressure; proBNP, brain natriuretic peptide pro-hormone; PVR, pulmonary vascular resistance; RAP, right atrial pressure; SSc, systemic sclerosis.

only (corresponding to Figure 3b) are provided in Tables S4 and S5. In both groups, RV mass metrics, including VMI, demonstrated the greatest magnitude of difference (of greatest significance) between subjects with versus without PAH.

ROC curves demonstrating CMR discrimination of subjects with versus without PAH are shown in Figure 4. The greatest AUC was for VMI [AUC 0.85 (95% CI: 0.78–0.93)]. All CMR metrics that differed significantly between subjects with versus without PAH (as shown in Figure 3a) were predictive of a diagnosis of PAH at RHC (Table 3). In both crude and adjusted regression, VMI had the greatest effect size among scaled variables. In univariable analysis, every 10% higher VMI (the unit change produced by log_{1.1} transformation) among subjects was associated with 52% greater odds of PAH at RHC (OR: 1.52, 95% CI: 1.25–1.84, *p* < 0.001). The next greatest effect size was for RVEF, for which each 10% decrease was associated with 38% greater odds of PAH

(OR: 0.62, 95% CI: 0.46–0.83, *p* < 0.001). In general, the magnitudes of effect sizes for univariable regressions were similar to those of multivariable regressions adjusted for age, sex, and PAH subtype, also shown in Table 3. In sensitivity analyses examining CMR discrimination of subjects with mild PAH only (subjects with mPAP 21–35 mmHg), VMI again demonstrated the greatest AUC (Figure S1) and the greatest effect size among scaled CMR variables in logistic regressions (Table S6).

When candidate logistic regression models with various possible combinations of predictive CMR metrics were tested and compared in the overall cohort, VMI, RV mass index (RVMI), RV end-diastolic volume index (RVEDVI), and RVFAC were identified as the subset of variables most predictive of PAH in the overall cohort. The ROC curve for this final multivariable logistic regression model for the overall cohort is shown in Figure 5a, with AUC 0.93 (95% CI:

TABLE 2 CMR Characteristics in Subjects with and without PAH

Observations, <i>n</i>	Measurement	No PAH	PAH	<i>p</i> value
89	RVEDV, mL	129 (37)	166 (59)	<0.01
88	RVEDVI, ml/m ²	73 (18)	91 (32)	<0.01
89	RVESV, ml	58 (22)	98 (55)	<0.01
88	RVESVI, ml/m ²	33 (11)	54 (31)	<0.01
89	RVM, g	32 (14)	59 (33)	<0.01
88	RVMI, g/m ²	18 (7)	33 (19)	<0.01
89	RVEF %	53 (12)	44 (13)	<0.01
69	TAPSE, mm	19 (5)	14 (6)	<0.01
89	VMI	0.29 (0.07)	0.53 (0.26)	<0.01
69	RVFS, %	22 (5)	15 (6)	<0.01
69	RVFAC, %	22 (4)	16 (6)	<0.01
89	RVMVR	0.25 (0.09)	0.37 (0.19)	<0.01
89	LVEDV, ml	114 (33)	105 (29)	0.23
88	LVEDVI, ml/m ²	64 (18)	57 (15)	0.06
89	LVESV, ml	41 (16)	39 (14)	0.57
88	LVESVI, ml/m ²	23 (9)	21 (7)	0.34
89	LVEDM, g	109 (32)	109 (29)	0.96
88	LVEDMI, g/m ²	62 (18)	61 (17)	0.65
85	LVESM, g	113 (33)	113 (27)	0.88
84	LVESMI, g/m ²	64 (17)	63 (16)	0.79

Note: All values reported as mean (SD) unless otherwise specified. *p* values correspond to significance testing of differences of means or medians as specified.

Abbreviations: EF, ejection fraction; LV, left ventricular; LVEDMI, left ventricular end diastolic mass index; LVEDVI, left ventricular end diastolic volume index; LVESMI, left ventricular end systolic mass index; LVESVI, left ventricular end systolic volume index; RV, right ventricular; RVEDVI, right ventricular end diastolic volume index; RVEF, right ventricular ejection fraction; RVESVI, right ventricular end systolic volume index; RVFAC, right ventricular fractional area change; RVFS, right ventricular fractional shortening; RVMI, right ventricular mass index; RVMVR, RV mass/volume ratio; TAPSE, tricuspid annular plane systolic excursion; VMI, ventricular mass index

0.87–0.99). In the subgroup of subjects with SSc, VMI, RVMI, RVEDVI, and tricuspid annular plane systolic excursion (TAPSE) were identified as the subset of variables most predictive of SSc-PAH. The ROC curve for this final multivariable logistic regression model for SSc is shown in Figure 5b, with AUC 0.94 (95% CI: 0.88–1.00). Both final predictive models were validated using leave-one-out cross-validation. The AUC for the cross-validated ROC curve for PAH for the overall cohort was 0.89 (95% CI: 0.82–0.97), while the AUC for the cross-validated ROC curve for SSc-PAH was 0.91 (95% CI: 0.82–1.00).

We examined RV end-systolic mass (RVESM) measurements, which, at our center, are inclusive of septomarginal and free wall trabeculations, in several exploratory analyses (Tables S7–S11). In contrast to

our RV end-diastolic mass (RVEDM) measurements, RVESM and RVESMI differed among subjects with mild versus moderate versus severe disease, with higher values in subjects with more severe disease. RVESM and RVESMI were also higher in IPAH compared to SSc-PAH. Both indexed and non-indexed RVESM measures performed similarly to RVEDM measures in logistic regression analysis, with each 10% increase in mass associated with 22%–24% greater odds of PAH. ROC comparisons demonstrated no differences in discrimination of PAH between RVESM and RVEDM measurements.

When relationships between VMI and RV loading conditions were explored, the nature of the relationship between VMI and PVR varied over the range of PVR measured in the cohort, with PVR ≤ 3 Wood units having

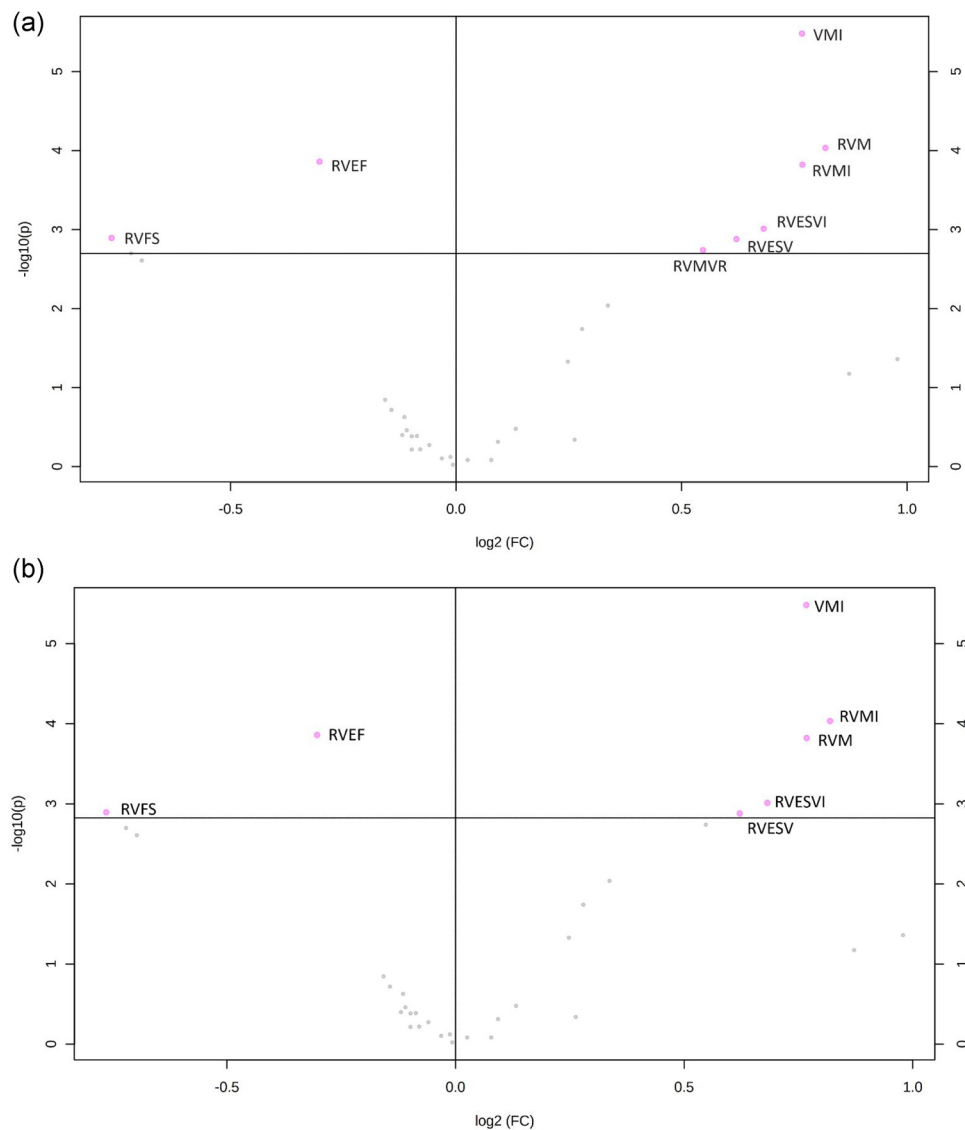


FIGURE 3 Volcano plots depicting the magnitude (expressed as \log_2 (fold change) on the x-axis) and significance (expressed as $-\log_{10}$ (p value) on the y axis) of differences in cardiac magnetic resonance metrics between subjects with versus without pulmonary arterial hypertension (PAH) in (a) the overall cohort and (b) the subset of subjects with systemic sclerosis. The position of each individual metric along the x and y axes is marked by a circle. Magenta circles denote metrics significantly different between subjects with versus without PAH after adjustment for multiple testing. Metrics that differ significantly in the overall cohort are labelled. The horizontal line represents the $-\log_{10}(p)$ threshold for statistical significance after Bonferroni correction for multiple comparisons ($p < 0.0015$)

no association with VMI, and $PVR > 3$ Wood units linearly associated with higher VMI (beta coefficient 0.03, 95% CI: 0.01–0.04, $p < 0.001$). VMI and RV mass increased linearly across the full range of mPAP in patients with PAH, including lower values of mPAP consistent with mild PAH. This is depicted in the scatter plots with superimposed lowess smoother lines in Figure S2. However, RV volumes did not relate linearly with lower values of mPAP consistent with mild PAH, and only began to rise at elevated mPAP measurements >35 – 60 mmHg (Figure S2). Similarly, measures of RV function, such as RVEF, RVFAC, RVFS, and TAPSE,

only began to fall with elevated mPAP >35 – 60 mmHg (Figure S2).

Relationships between VMI and other CMR metrics predictive of PAH were explored, and scatter plots with superimposed lowess smoother lines depicting these relationships in PAH are shown in Figure S3. Aside from RV mass metrics, other predictive metrics reflecting RV volumes or function had inconsistent relationships with lower values of VMI, and did not begin to linearly associate until VMI measurements of 0.3–0.4 were reached. Up to VMI measurements of 0.37 (the median VMI for the overall

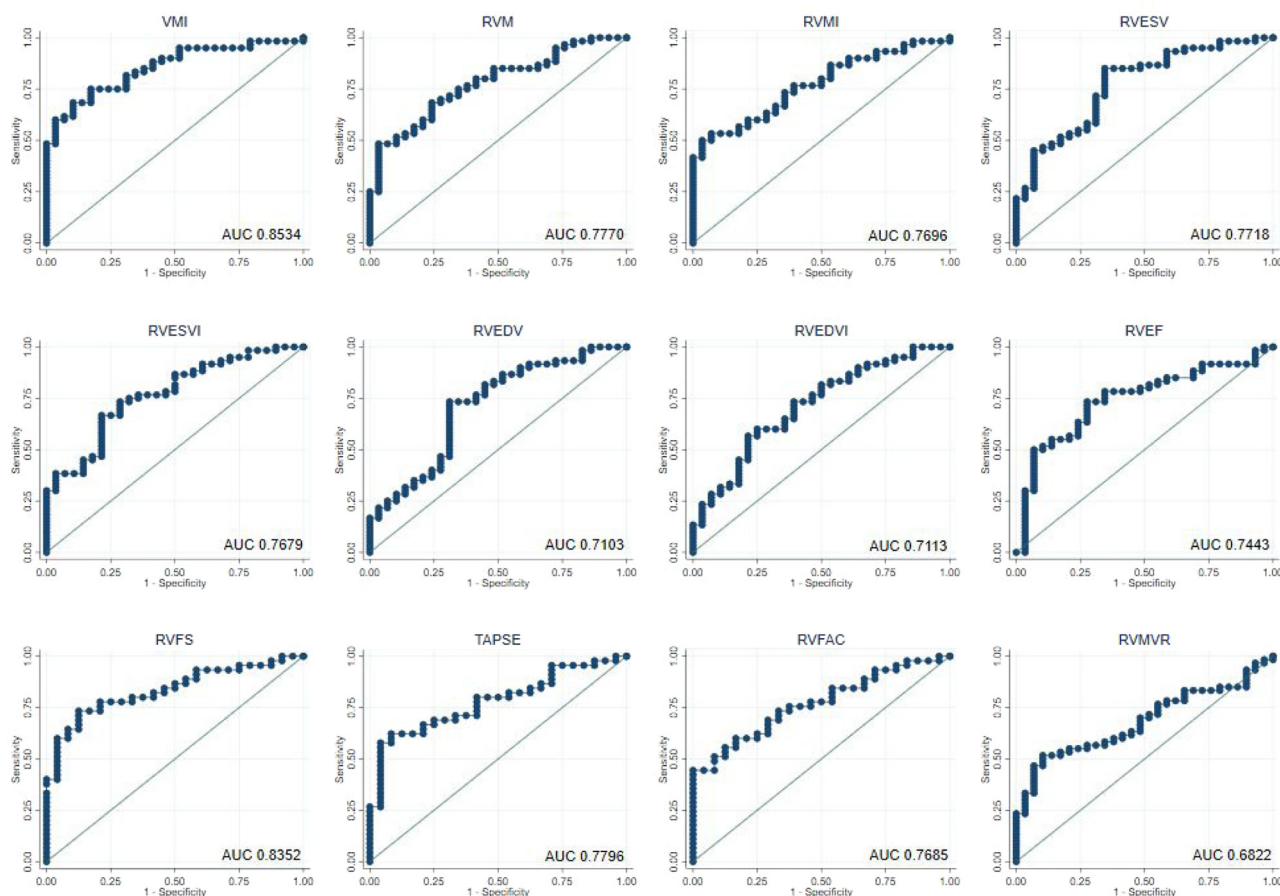


FIGURE 4 Receiver operating characteristic curves for CMR metrics that differ in subjects with versus without PAH in the overall cohort. CMR, cardiac magnetic resonance; PAH, pulmonary arterial hypertension; RV, right ventricular; RVEDV, RV end-diastolic volume; RVEDVI, RV end-diastolic volume index; RVEF, RV ejection fraction; RVESV, RV end-systolic volume; RVESVI, RV end-systolic volume index; RVFAC, RV fractional area change; RVFS, RV fractional shortening; RVM, RV mass; RVMI, RV mass index; RVMVR, RV mass/volume ratio; TAPSE, tricuspid annular plane systolic excursion; VMI, ventricular mass index

CMR metric	Crude			Adjusted ^a		
	OR	95% CI	<i>p</i> value	OR	95% CI	<i>p</i> value
VMI	1.52	1.25, 1.84	<0.001	1.54	1.25, 1.91	<0.001
RVM, g	1.23	1.11, 1.37	<0.001	1.27	1.13, 1.43	<0.001
RVMI, g/m ²	1.20	1.09, 1.33	<0.001	1.24	1.11, 1.39	<0.001
RVESV, ml	1.29	1.12, 1.48	<0.001	1.38	1.16, 1.65	<0.001
RVESVI, ml/m ²	1.30	1.12, 1.50	<0.001	1.38	1.15, 1.66	0.001
RVFS, %	0.68	0.54, 0.86	0.001	0.70	0.55, 0.88	0.002
RVEF, %	0.62	0.46, 0.83	<0.001	0.60	0.44, 0.83	0.002
RVMVR	1.14	1.03, 1.25	0.007	1.16	1.04, 1.28	0.005

TABLE 3 Crude and adjusted odds of PAH for CMR metrics

Note: All metrics are scaled to log_{1,1} to facilitate direct comparisons of effect sizes. See Table 2 for abbreviations.

^aAdjusted for age, sex, and SSc-PAH versus IPAH.

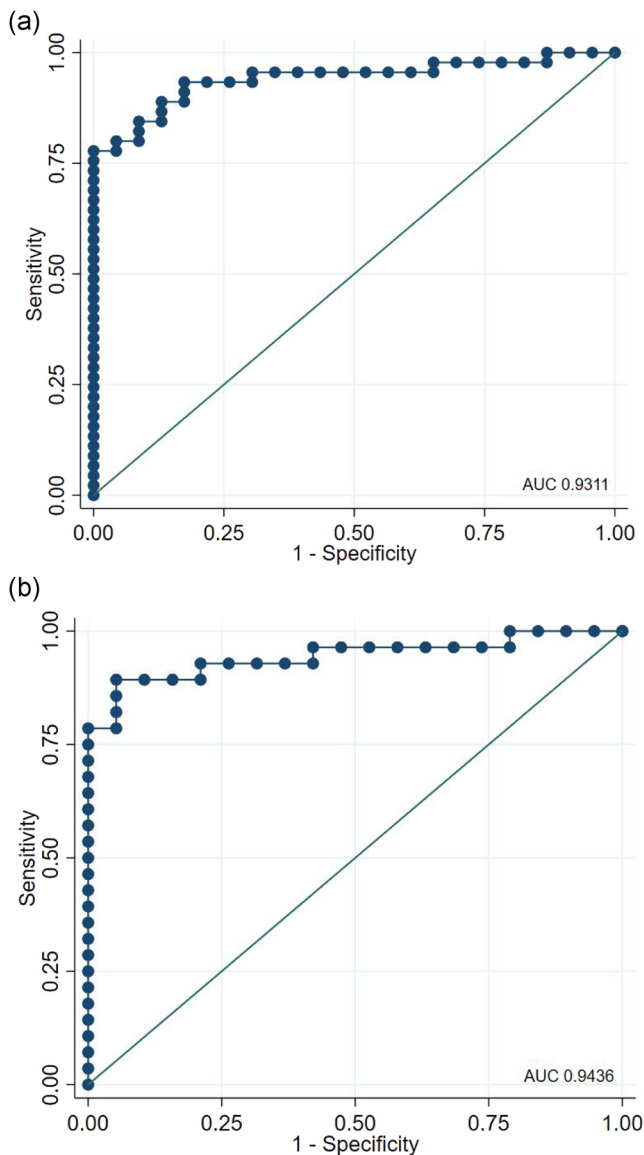


FIGURE 5 Receiver operating characteristic curves corresponding to the final predictive multivariable logistic regression models in (a) the overall cohort, with best subset predictors ventricular mass index (VMI), right ventricular (RV) end-diastolic mass index (RVEDMI), RV end-diastolic volume index (RVEDVI), and RV fractional area change (RVFAC) included; and (b) the subgroup of subjects with SSc, with best subset predictors VMI, RV mass index (RVMI), RV end-diastolic volume index (RVEDVI), and tricuspid annular plane systolic excursion (TAPSE) included

cohort and the 25th percentile for those with SSc-PAH), no relationship existed between higher VMI and several other metrics predictive of PAH, such as RVEF, TAPSE, or RV volumes, which remained in normal ranges. For the overall cohort, $VMI \geq 0.37$ was 73% sensitive and 83% specific for PAH, with a PPV of 90% and a negative predictive value of 61%.

DISCUSSION

Our results demonstrate that CMR measures of RV mass, particularly VMI, are predictors of mild, incident PAH in this prospectively enrolled cohort of patients deemed at risk for or suspected of disease by their treating clinicians. For every 10% increase in VMI on CMR, odds of a new diagnosis of PAH increased by 54%, and $VMI \geq 0.37$ yielded a 90% PPV for PAH defined by 6th WSPH criteria. Among the available measurements, VMI and RV mass metrics demonstrated the greatest magnitude difference in patients with PAH compared to those without PAH at RHC. Furthermore, our results show that VMI, in contrast with other predictive CMR metrics, is linearly associated with lower mPAP measurements, including the range of values representing a group of subjects who meet revised diagnostic criteria for PAH. Taken together, these results suggest VMI may be an early marker of PAH in at-risk populations similar to the study cohort. To our knowledge, our results are the first to demonstrate the value of RV mass metrics, particularly VMI, in at-risk subjects diagnosed with mild PAH in particular, including those with PAH as redefined by 6th WSPH hemodynamic criteria.

Our results are in alignment with previous studies of CMR metrics in PAH that have found value in VMI. We and others have previously shown that VMI is predictive of clinical outcomes, including mortality.^{15,28,29} In 2009, Hagger et al. found VMI was strongly correlated with mPAP and predictive of the presence of PAH, with a VMI threshold of 0.56 yielding a PPV of 88% in SSc patients with suspected PAH referred for RHC.¹³ This was a small cohort, with 28 patients diagnosed with SSc-PAH at RHC performed within 30 days of CMR. In 2019, a larger retrospective study by Johns et al. reported VMI was one of three variables (along with interventricular septal angle and black blood slow flow score) incorporated into a multivariable regression model yielding high diagnostic accuracy for PAH.¹⁴ These prior studies, however, examined diagnostic accuracy for an mPAP threshold of 25 mmHg for PAH, and they did not specifically examine the ability of CMR metrics to predict mild PAH. Only one CMR study investigated metrics discriminating mild PAH specifically (defined by the authors as mPAP 25–40 mmHg) from healthy controls. This study found PA pulsatility distinguished mild PAH from controls, but found no differences in conventional RV volume, mass, or functional metrics between these two groups.³⁰ Notably, VMI was not assessed. In 2020, the prior analysis by Johns et al. was updated for the new diagnostic threshold for PAH and reconfirmed VMI as one of the best discriminators of disease.²¹ Authors did not examine patients with mild PAH specifically, however, and

because healthy controls were used as comparators, this cohort did not reflect an “at-risk” population generalizable to patients referred for screening.

Controversy exists over how best to screen for PAH. Currently utilized screening algorithms, such as the DETECT algorithm³¹ or European Society of Cardiology/European Respiratory Society guidelines,³² do not include CMR, and no clear consensus exists regarding use of CMR metrics for diagnostic or screening purposes. Echocardiography is typically incorporated into screening strategies for suspected PAH,^{31,32} however, there is poor agreement between echocardiographically estimated pressures and invasively measured pressures at RHC.³³ Furthermore, arriving at an echocardiographic estimate of pulmonary artery pressure requires a tricuspid regurgitant jet, which is not always present or visualized, and a gross estimate of right atrial pressure, which is based on visual inspection of collapsibility of the inferior vena cava.³⁴ A comparison of the diagnostic and prognostic utility of CT, MRI, and echocardiographic measurements in one study of patients with connective tissue disease (the majority of whom had SSc) showed baseline CMR measurements outperformed echocardiographic measurements for predicting mortality.¹⁵ Importantly, our study cohort was composed of a large proportion (72%) of patients with SSc, the population in which PAH screening is most commonly undertaken. Our SSc subgroup analyses show that VMI and RV mass are significantly higher in SSc patients with versus without PAH, and also show that VMI is one of the most discriminatory CMR variables for detecting SSc-PAH. Given the disproportionate morbidity and mortality suffered by patients with SSc-PAH,^{35,36} identification of CMR metrics able to detect early, mild disease could have important screening implications.

Most previous CMR studies in PAH have focused on the prognostic value of measures of RV volumes or RVEF, and fewer studies have highlighted the relevance of mass-based metrics. RV volumes and RVEF are intuitive surrogates for RV dilatation and dysfunction, which generally represent more severe disease. Clinically, RV dilatation and dysfunction in PAH are typically preceded by RV hypertrophy, which is thought to occur early in disease as an adaptive response to increased RV afterload.^{37–39} Our results reflect this, as we found that in PAH subjects with only mildly elevated mPAP, RV mass measurements were high, while RV volume and functional measurements tended to be normal. This typical progression of morphologic RV change, with hypertrophy occurring early in disease, highlights the importance of RV mass measurements when CMR is utilized for screening or diagnostic purposes. In our cohort, VMI measurements predictive of PAH were

associated with RV volume and functional measures still in the normal range.

Some unique aspects of how VMI is derived may position this measure as a particularly useful mass metric. There may be value in incorporating LV mass into assessments of RV adaptation. In PAH, the pressure-overloaded RV bows into the LV, under-filling and unloading the LV, leading to atrophic LV remodeling.^{40,41} By including LV mass in the measure, VMI may thus reflect a pattern of RV geometric change specific to PAH pathobiology. Additionally, prior work in CMR has shown that indexing mass and volume metrics to body surface area improves the prognostic value of these metrics.⁴² Moreover, expressing these indexed metrics in terms of percent-predicted values, compared against expected values for normal subjects of the same age and sex, improves prognostic value further.^{42–44} However, CMR readers rarely report measurements in this fashion. By measuring RV mass against LV mass, both commonly reported, VMI effectively indexes each patient to him or herself. With larger studies, VMI may prove to be a more meaningful metric than RV mass alone. Our exploratory analyses of RVESM measurements do not demonstrate conclusive benefit to including RV trabeculations in RV mass measurements. Although differences not seen in RVEDM do exist in RVESM measurements across categories of disease severity and between IPAH and SSc-PAH, the significance of these differences is unclear. AUCs for RVESM measures are higher than those for RVEDM in absolute terms, though ROC comparisons do not show any significant differences in discrimination.

Our study is strengthened by the prospective nature of enrollment, access to a real-world population of treatment-naïve patients at risk of disease, including many with SSc referred by rheumatologists, and careful and multi-disciplinary phenotyping of patients. There was minimal missing data. Additionally, in accordance with the pre-determined study protocol, the allowable period between CMR and RHC was constrained to 48 h (with 86% of subjects undergoing both studies within 24 h), limiting time for any changes in cardiopulmonary physiology to occur between tests. No changes in medical management were made between tests. However, the study has some limitations. It is a single-center study of a cohort enriched for SSc, and the composition of the cohort may limit the generalizability of our findings to other screening populations. Though we performed internal cross-validation, results are not externally validated. The change in WSPH diagnostic criteria only affected whether PAH was diagnosed by RHC in a small number of study participants with mPAP in the 21–24 mmHg range, however, our sensitivity analyses demonstrated consistency and robustness of the key findings in subjects with mild PAH with mPAP \leq 35 mmHg. Some

CMR metrics, such as PA area and compliance, intraventricular septal angle, or black blood score, were not captured and not available for discriminatory analysis. Finally, there may be an intrinsic cost limitation to the potential use of CMR as a screening tool. However, MRI is currently utilized to screen for diseases that confer substantially lower mortality than SSc-PAH, such as early-stage breast cancer, in at-risk populations with disease incidence comparable to that of PAH in SSc.^{45,46}

In conclusion, VMI and other RV mass metrics measured by CMR are predictors of mild, RHC-confirmed PAH using the lower diagnostic threshold established by the 6th WSPH. Additional studies are needed to validate these findings in larger cohorts of patients found to have mild disease, to compare CMR-based screening directly to other commonly utilized screening protocols, and to assess the supplemental detection yield gained by adding CMR to existing protocols. In contrast to prior studies, future CMR studies should focus especially on measures capable of discriminating early, mild PAH from similar subjects also at high risk of disease. This will be particularly true if clinical trials currently underway show that treatment of PAH patients with mPAP in the 21–24 mmHg range slows disease progression or brings about a survival benefit. In addition to the focus on RV volume measures and RVEF, clinicians should attend to mass-based metrics, such as VMI, when interpreting results of CMR exams, particularly in patients undergoing evaluation of possible PAH.

ACKNOWLEDGMENT

Supported, in part, by National Institutes of Health K23HL153781 (CES), P50 HL084946, R01HL114910, and U01HL125175 (PMH).

CONFLICT OF INTERESTS

The authors declare that there are no conflict of interests.

ETHICS STATEMENT

The authors confirm that the ethical policies of the journal, as noted on the journal's author guidelines page, have been adhered to and the appropriate ethical review committee approval has been received.

AUTHOR CONTRIBUTIONS

Study design: Catherine E. Simpson, Rachel L. Damico, and Paul M. Hassoun. *Patient recruitment, care, and follow-up:* Rachel L. Damico, Todd M. Kolb, Steven Hsu, Stephen C. Mathai, and Paul M. Hassoun. *Data collection, maintenance, and analysis:* Catherine E. Simpson, Steven Hsu, Rachel L. Damico. *CMR interpretation:* Stefan L. Zimmerman, Celia P. Corona-Villalobos. *Statistical analyses:* Catherine E. Simpson and Rachel L. Damico. *Drafted*

the manuscript: Catherine E. Simpson. *Critical revision of the manuscript for important intellectual content:* Rachel L. Damico, Stephen C. Mathai, Todd M. Kolb, and Paul M. Hassoun.

ORCID

Catherine E. Simpson  <http://orcid.org/0000-0002-2388-5660>

REFERENCES

1. Maron BA, Abman SH, Elliott CG, Frantz RP, Hopper RK, Horn EM, Nicolls MR, Shlobin OA, Shah SJ, Kovacs G, Olschewski H, Rosenzweig EB. Pulmonary arterial hypertension: diagnosis, treatment, and novel advances. *Am J Respir Crit Care Med.* 2021;203:1472–87. <https://doi.org/10.1164/rccm.202012-4317SO>
2. Simonneau G, Montani D, Celermajer DS, Denton CP, Gatzoulis MA, Krowka M, Williams PG, Souza R. Haemodynamic definitions and updated clinical classification of pulmonary hypertension. *Eur Respir J.* 2019;53:1801913. <https://doi.org/10.1183/13993003.01913-2018>
3. Lewis RA, Johns CS, Cogliano M, Capener D, Tubman E, Elliot CA, Charalampopoulos A, Sabroe I, Thompson A, Billings CG, Hamilton N, Baster K, Laud PJ, Hickey PM, Middleton J, Armstrong IJ, Hurdman JA, Lawrie A, Rothman A, Wild JM, Condliffe R, Swift AJ, Kiely DG. Identification of cardiac magnetic resonance imaging thresholds for risk stratification in pulmonary arterial hypertension. *Am J Respir Crit Care Med.* 2020;201:458–68. <https://doi.org/10.1164/rccm.201909-1771OC>
4. Inampudi C, Tedford RJ, Hemnes AR, Hansmann G, Bogaard HJ, Koestenberger M, Lang IM, Brittain EL. Treatment of right ventricular dysfunction and heart failure in pulmonary arterial hypertension. *Cardiovasc Diagn Ther.* 2020;10:1659–74. <https://doi.org/10.21037/cdt-20-348>
5. Kovács A, Lakatos B, Tokodi M, Merkely B. Right ventricular mechanical pattern in health and disease: beyond longitudinal shortening. *Heart Fail Rev.* 2019;24:511–20. <https://doi.org/10.1007/s10741-019-09778-1>
6. van de Veerdonk MC, Kind T, Marcus JT, Mauritz GJ, Heymans MW, Bogaard HJ, Boonstra A, Marques KM, Westerhof N, Vonk-Noordegraaf A. Progressive right ventricular dysfunction in patients with pulmonary arterial hypertension responding to therapy. *J Am Coll Cardiol.* 2011;58:2511–9. <https://doi.org/10.1016/j.jacc.2011.06.068>
7. Lahm T, Douglas IS, Archer SL, Bogaard HJ, Chesler NC, Haddad F, Hemnes AR, Kawut SM, Kline JA, Kolb TM, Mathai SC, Mercier O, Michelakis ED, Naeije R, Tuder RM, Ventetuolo CE, Vieillard-Baron A, Voelkel NF, Vonk-Noordegraaf A, Hassoun PM, American Thoracic Society Assembly on Pulmonary C. Assessment of right ventricular function in the research setting: knowledge gaps and pathways forward. an official american thoracic society research statement. *Am J Respir Crit Care Med.* 2018;198:e15–43. <https://doi.org/10.1164/rccm.201806-1160ST>
8. Mooij CF, de Wit CJ, Graham DA, Powell AJ, Geva T. Reproducibility of MRI measurements of right ventricular size and function in patients with normal and dilated ventricles.

- J Magn Reson Imaging. 2008;28:67–73. <https://doi.org/10.1002/jmri.21407>
9. Peacock AJ, Crawley S, McLure L, Blyth KG, Vizza CD, Poscia R, Francone M, Iacucci I, Olschewski H, Kovacs G, Vonk Noordegraaf A, Marcus JT, van de Veerdonk MC, Oosterveer FP. Changes in right ventricular function measured by cardiac magnetic resonance imaging in patients receiving pulmonary arterial hypertension-targeted therapy: the EURO-MR study. *Circ Cardiovasc Imaging*. 2014;7:107–14. <https://doi.org/10.1161/CIRCIMAGING.113.000629>
 10. Baggen VJ, Leiner T, Post MC, van Dijk AP, Roos-Hesselink JW, Boersma E, Habets J, Sieswerda GT. Cardiac magnetic resonance findings predicting mortality in patients with pulmonary arterial hypertension: a systematic review and meta-analysis. *Eur Radiol*. 2016;26:3771–80. <https://doi.org/10.1007/s00330-016-4217-6>
 11. Dong Y, Pan Z, Wang D, Lv J, Fang J, Xu R, Ding J, Cui X, Xie X, Wang X, Chen Md Y, Guo X. Prognostic value of cardiac magnetic resonance-derived right ventricular remodeling parameters in pulmonary hypertension: a systematic review and meta-analysis. *Circ Cardiovasc Imaging*. 2020;13:e010568. <https://doi.org/10.1161/CIRCIMAGING.120.010568>
 12. Alabed S, Shahin Y, Garg P, Alandejani F, Johns CS, Lewis RA, Condliffe R, Wild JM, Kiely DG, Swift AJ. Cardiac-MRI predicts clinical worsening and mortality in pulmonary arterial hypertension: a systematic review and meta-analysis. *JACC Cardiovasc Imaging*. 2021;14:931–42. <https://doi.org/10.1016/j.jcmg.2020.08.013>
 13. Hagger D, Condliffe R, Woodhouse N, Elliot CA, Armstrong IJ, Davies C, Hill C, Akil M, Wild JM, Kiely DG. Ventricular mass index correlates with pulmonary artery pressure and predicts survival in suspected systemic sclerosis-associated pulmonary arterial hypertension. *Rheumatology (Oxford)*. 2009;48:1137–42. <https://doi.org/10.1093/rheumatology/kep187>
 14. Johns CS, Kiely DG, Rajaram S, Hill C, Thomas S, Karunasaagarar K, Garg P, Hamilton N, Solanki R, Capener DA, Elliot C, Sabroe I, Charalamopoulos A, Condliffe R, Wild JM, Swift AJ. Diagnosis of pulmonary hypertension with cardiac MRI: derivation and validation of regression models. *Radiology*. 2019;290:61–8. <https://doi.org/10.1148/radiol.2018180603>
 15. Rajaram S, Swift AJ, Capener D, Elliot CA, Condliffe R, Davies C, Hill C, Hurdman J, Kidling R, Akil M, Wild JM, Kiely DG. Comparison of the diagnostic utility of cardiac magnetic resonance imaging, computed tomography, and echocardiography in assessment of suspected pulmonary arterial hypertension in patients with connective tissue disease. *J Rheumatol*. 2012;39:1265–74. <https://doi.org/10.3899/jrheum.110987>
 16. Swift AJ, Lu H, Uthoff J, Garg P, Cogliano M, Taylor J, Metherall P, Zhou S, Johns CS, Alabed S, Condliffe RA, Lawrie A, Wild JM, Kiely DG. A machine learning cardiac magnetic resonance approach to extract disease features and automate pulmonary arterial hypertension diagnosis. *Eur Heart J Cardiovasc Imaging*. 2020;22:236–45. <https://doi.org/10.1093/ehjci/jeaa001>
 17. Swift AJ, Rajaram S, Condliffe R, Capener D, Hurdman J, Elliot C, Kiely DG, Wild JM. Pulmonary artery relative area change detects mild elevations in pulmonary vascular resistance and predicts adverse outcome in pulmonary hypertension. *Invest Radiol*. 2012;47:571–7. <https://doi.org/10.1097/RLI.0b013e31826c4341>
 18. Swift AJ, Rajaram S, Marshall H, Condliffe R, Capener D, Hill C, Davies C, Hurdman J, Elliot CA, Wild JM, Kiely DG. Black blood MRI has diagnostic and prognostic value in the assessment of patients with pulmonary hypertension. *Eur Radiol*. 2012;22:695–702. <https://doi.org/10.1007/s00330-011-2306-0>
 19. Douschan P, Kovacs G, Avian A, Foris V, Gruber F, Olschewski A, Olschewski H. Mild elevation of pulmonary arterial pressure as a predictor of mortality. *Am J Respir Crit Care Med*. 2018;197:509–16. <https://doi.org/10.1164/rccm.201706-1215OC>
 20. Kovacs G, Berghold A, Scheidl S, Olschewski H. Pulmonary arterial pressure during rest and exercise in healthy subjects: a systematic review. *Eur Respir J*. 2009;34:888–94. <https://doi.org/10.1183/09031936.00145608>
 21. Whitfield AJ, Solanki R, Johns CS, Kiely D, Wild J, Swift AJ. MRI prediction of precapillary pulmonary hypertension according to the Sixth World Symposium on pulmonary hypertension. *Radiology*. 2020;294:482. <https://doi.org/10.1148/radiol.2019192078>
 22. Hachulla E, Gressin V, Guillevin L, Carpentier P, Diot E, Sibilia J, Kahan A, Cabane J, Francès C, Launay D, Mouthon L, Allanore Y, Tiev KP, Cleron P, de Groote P, Humbert M. Early detection of pulmonary arterial hypertension in systemic sclerosis: a French nationwide prospective multicenter study. *Arthritis Rheum*. 2005;52:3792–800. <https://doi.org/10.1002/art.21433>
 23. Humbert M, Yaici A, de Groote P, Montani D, Sitbon O, Launay D, Gressin V, Guillevin L, Cleron P, Simonneau G, Hachulla E. Screening for pulmonary arterial hypertension in patients with systemic sclerosis: clinical characteristics at diagnosis and long-term survival. *Arthritis Rheum*. 2011;63:3522–30. <https://doi.org/10.1002/art.30541>
 24. Steen V, Medsger TA Jr. Predictors of isolated pulmonary hypertension in patients with systemic sclerosis and limited cutaneous involvement. *Arthritis Rheum*. 2003;48:516–22. <https://doi.org/10.1002/art.10775>
 25. Simpson CE, Damico RL, Hummers L, Khair RM, Kolb TM, Hassoun PM, Mathai SC. Serum uric acid as a marker of disease risk, severity, and survival in systemic sclerosis-related pulmonary arterial hypertension. *Pulm Circ*. 2019;9:2045894019859477. <https://doi.org/10.1177/2045894019859477>
 26. Corona-Villalobos CP, Kamel IR, Rastegar N, Damico R, Kolb TM, Boyce DM, Sager AE, Skrok J, Shehata ML, Vogel-Claussen J, Bluemke DA, Girgis RE, Mathai SC, Hassoun PM, Zimmerman SL. Bidimensional measurements of right ventricular function for prediction of survival in patients with pulmonary hypertension: comparison of reproducibility and time of analysis with volumetric cardiac magnetic resonance imaging analysis. *Pulm Circ*. 2015;5:527–37. <https://doi.org/10.1086/682229>
 27. Saba TS, Foster J, Cockburn M, Cowan M, Peacock AJ. Ventricular mass index using magnetic resonance imaging accurately estimates pulmonary artery pressure. *Eur Respir J*. 2002;20:1519–24.
 28. Yamada Y, Okuda S, Kataoka M, Tanimoto A, Tamura Y, Abe T, Okamura T, Fukuda K, Satoh T, Kuribayashi S.

- Prognostic value of cardiac magnetic resonance imaging for idiopathic pulmonary arterial hypertension before initiating intravenous prostacyclin therapy. *Circ J*. 2012;76:1737–43.
29. Simpson CE, Damico RL, Kolb TM, Mathai SC, Khair RM, Sato T, Bourji K, Tedford RJ, Zimmerman SL, Hassoun PM. Ventricular mass as a prognostic imaging biomarker in incident pulmonary arterial hypertension. *Eur Respir J*. 2019;53:1802067. <https://doi.org/10.1183/13993003.02067-2018>
 30. Ray JC, Burger C, Mergo P, Safford R, Blackshear J, Austin C, Fairweather D, Heckman MG, Zeiger T, Dubin M, Shapiro B. Pulmonary arterial stiffness assessed by cardiovascular magnetic resonance imaging is a predictor of mild pulmonary arterial hypertension. *Int J Cardiovasc Imaging*. 2019;35:1881–92. <https://doi.org/10.1007/s10554-018-1397-y>
 31. Coghlan JG, Denton CP, Grünig E, Bonderman D, Distler O, Khanna D, Müller-Ladner U, Pope JE, Vonk MC, Doelberg M, Chadha-Boreham H, Heinzl H, Rosenberg DM, McLaughlin VV, Seibold JR, on Behalf of the DETECT Study Group. Evidence-based detection of pulmonary arterial hypertension in systemic sclerosis: the DETECT study. *Ann Rheum Dis*. 2014;73:1340–9. <https://doi.org/10.1136/annrheumdis-2013-203301>
 32. Galiè N, Humbert M, Vachiery JL, Gibbs S, Lang I, Torbicki A, Simonneau G, Peacock A, Vonk Noordegraaf A, Beghetti M, Ghofrani A, Gomez Sanchez MA, Hansmann G, Klepetko W, Lancellotti P, Matucci M, McDonagh T, Pierard LA, Trindade PT, Zompatori M, Hoeper M. 2015 ESC/ERS Guidelines for the diagnosis and treatment of pulmonary hypertension: The Joint Task Force for the Diagnosis and Treatment of Pulmonary Hypertension of the European Society of Cardiology (ESC) and the European Respiratory Society (ERS): Endorsed by: Association for European Paediatric and Congenital Cardiology (AEPC), International Society for Heart and Lung Transplantation (ISHLT). *Eur Respir J*. 2015;46:903–75. <https://doi.org/10.1183/13993003.01032-2015>
 33. Fisher MR, Forfia PR, Chamera E, Housten-Harris T, Champion HC, Girgis RE, Corretti MC, Hassoun PM. Accuracy of Doppler echocardiography in the hemodynamic assessment of pulmonary hypertension. *Am J Respir Crit Care Med*. 2009;179:615–21. <https://doi.org/10.1164/rccm.200811-1691OC>
 34. Lang RM, Badano LP, Mor-Avi V, Afilalo J, Armstrong A, Ernande L, Flachskampf FA, Foster E, Goldstein SA, Kuznetsova T, Lancellotti P, Muraru D, Picard MH, Rietzschel ER, Rudski L, Spencer KT, Tsang W, Voigt JU. Recommendations for cardiac chamber quantification by echocardiography in adults: an update from the American Society of Echocardiography and the European Association of Cardiovascular Imaging. *J Am Soc Echocardiogr*. 2015;28:1–39.e14. <https://doi.org/10.1016/j.echo.2014.10.003>
 35. Chaisson NF, Hassoun PM. Systemic sclerosis-associated pulmonary arterial hypertension. *Chest*. 2013;144:1346–56. <https://doi.org/10.1378/chest.12-2396>
 36. Chung L, Domsic RT, Lingala B, Alkassab F, Bolster M, Csuka ME, Derk C, Fischer A, Frech T, Furst DE, Gombert-Maitland M, Hinchcliff M, Hsu V, Hummers LK, Khanna D, Medsger TA Jr, Molitor JA, Preston IR, Schioppa E, Shapiro L, Silver R, Simms R, Varga J, Gordon JK, Steen VD. Survival and predictors of mortality in systemic sclerosis-associated pulmonary arterial hypertension: outcomes from the pulmonary hypertension assessment and recognition of outcomes in scleroderma registry. *Arthritis Care Res (Hoboken)*. 2014;66:489–95. <https://doi.org/10.1002/acr.22121>
 37. Haddad F, Doyle R, Murphy DJ, Hunt SA. Right ventricular function in cardiovascular disease, part II: pathophysiology, clinical importance, and management of right ventricular failure. *Circulation*. 2008;117:1717–31. <https://doi.org/10.1161/CIRCULATIONAHA.107.653584>
 38. Haddad F, Hunt SA, Rosenthal DN, Murphy DJ. Right ventricular function in cardiovascular disease, part I: anatomy, physiology, aging, and functional assessment of the right ventricle. *Circulation*. 2008;117:1436–48. <https://doi.org/10.1161/CIRCULATIONAHA.107.653576>
 39. Vonk-Noordegraaf A, Haddad F, Chin KM, Forfia PR, Kawut SM, Lumens J, Naeije R, Newman J, Oudiz RJ, Provencher S, Torbicki A, Voelkel NF, Hassoun PM. Right heart adaptation to pulmonary arterial hypertension: physiology and pathobiology. *J Am Coll Cardiol*. 2013;62:D22–33. <https://doi.org/10.1016/j.jacc.2013.10.027>
 40. Marcus JT, Gan CT, Zwanenburg JJ, Boonstra A, Allaart CP, Götte MJ, Vonk-Noordegraaf A. Interventricular mechanical asynchrony in pulmonary arterial hypertension: left-to-right delay in peak shortening is related to right ventricular overload and left ventricular underfilling. *J Am Coll Cardiol*. 2008;51:750–7. <https://doi.org/10.1016/j.jacc.2007.10.041>
 41. Vonk-Noordegraaf A, Marcus JT, Gan CT, Boonstra A, Postmus PE. Interventricular mechanical asynchrony due to right ventricular pressure overload in pulmonary hypertension plays an important role in impaired left ventricular filling. *Chest*. 2005;128:628S–30S. https://doi.org/10.1378/chest.128.6_suppl.628S
 42. Maceira AM, Prasad SK, Khan M, Pennell DJ. Reference right ventricular systolic and diastolic function normalized to age, gender and body surface area from steady-state free precession cardiovascular magnetic resonance. *Eur Heart J*. 2006;27:2879–88. <https://doi.org/10.1093/eurheartj/ehl336>
 43. Swift AJ, Rajaram S, Campbell MJ, Hurdman J, Thomas S, Capener D, Elliot C, Condliffe R, Wild JM, Kiely DG. Prognostic value of cardiovascular magnetic resonance imaging measurements corrected for age and sex in idiopathic pulmonary arterial hypertension. *Circ Cardiovasc Imaging*. 2014;7:100–6. <https://doi.org/10.1161/CIRCIMAGING.113.000338>
 44. Kawut SM, Lima JA, Barr RG, Chahal H, Jain A, Tandri H, Praestgaard A, Bagiella E, Kizer JR, Johnson WC, Kronmal RA, Bluemke DA. Sex and race differences in right ventricular structure and function: the multi-ethnic study of atherosclerosis-right ventricle study. *Circulation*. 2011;123:2542–51. <https://doi.org/10.1161/Circulationaha.110.985515>
 45. Lord SJ, Lei W, Craft P, Cawson JN, Morris I, Walleiser S, Griffiths A, Parker S, Houssami N. A systematic review of the effectiveness of magnetic resonance imaging (MRI) as an addition to mammography and ultrasound in screening young women at high risk of breast cancer. *Eur J Cancer*. 2007;43:1905–17. <https://doi.org/10.1016/j.ejca.2007.06.007>
 46. Berg WA, Zhang Z, Lehrer D, Jong RA, Pisano ED, Barr RG, Böhm-Vélez M, Mahoney MC, Evans WP, Larsen LH, Morton MJ, Mendelson EB, Farria DM,

Cormack JB, Marques HS, Adams A, Yeh NM, Gabrielli G, ACRIN I. Detection of breast cancer with addition of annual screening ultrasound or a single screening MRI to mammography in women with elevated breast cancer risk. *JAMA*. 2012;307:1394–404. <https://doi.org/10.1001/jama.2012.388>

SUPPORTING INFORMATION

Additional supporting information may be found in the online version of the article at the publisher's website.

How to cite this article: Simpson CE, Kolb TM, Hsu S, Zimmerman SL, Corona-Villalobos CP, Mathai SC, Damico RL, Hassoun PM. Ventricular mass discriminates pulmonary arterial hypertension as redefined at the Sixth World Symposium on Pulmonary Hypertension. *Pulmonary Circulation*. 2022;12:e12005. <https://doi.org/10.1002/pul2.12005>